Outgassing and Vaporization Considerations in MilliWatt Generators Designed for 20-Year Missions

Nathan Hiller[1], Daniel Allen[1], Norbert Elsner[1], J. C. Bass[1], and J. Peyton Moore[2]

[1] Hi-Z Technology Inc., 7606 Miramar Road, Suite 7400, San Diego, CA 92126
[2] Radioisotope Power Systems Program, MS 6080, Bldg. 4508, Rm. 264, Oak Ridge National Laboratory, Oak Ridge, TN 37831
858-695-6660; nhiller@hi-z.com

Abstract. Ongoing experimental work and theoretical models indicate that milliwatt thermoelectric generators that operate in a sealed-off vacuum environment will be useful for long-term operation, such as the PASCAL 20 year Mars mission and the CryoScout mission. Considerations for long-term operation include out gassing of the multifoil vacuum insulation before pinch off and vaporization of the $(Bi,Sb)_2(Se,Te)_3$ thermoelectric materials during long-term operation. Tests underway indicate the multi-foil insulation can be pre-outgassed before assembly so further outgassing in the sealed generator is minimized. Experimental data and vaporization models for a Th of 250 °C thus far indicate that the small amount of vaporization of materials used in the thermoelectric module do not significantly effect the generator vacuum or the module power output. These tests and models indicate that both potential modes of degradation can be controlled and minimized. Although performance data on the generator materials only extend for several hundred hours, the good performances in a limited time, combined with an understanding of the materials behavior, indicate that milliwatt generator holds promise for providing sufficient and reliable power for space missions lasting up to 20 years.

BACKGROUND

The PASCAL Mars Network Mission requires a 40 mW power source for each of the 24 surface climate-monitoring probes during a 20-year mission (Allen, 2001). The Jet Propulsion Laboratories Cryobot mission or Cryo-Hydro Integrated Robotic Penetrator System (CHIRPS) requires several 150 mW RTGs to power mini-radiowave ice transceivers for a one- to two-year mission (Zimmerman, 2001). The power requirements for these missions can probably be met using sealed-off vacuum RTGs that require a vacuum and multifoil insulation for maximum power output. However; sealed-off vacuum RTG's have not been used for any mission thus far. Reliability of sealed-off vacuum RTG's can be affected by the vaporization of the thermoelectric module and insulation residual outgassing. This paper addresses both areas of concern.

The power output of the RTG is dependent upon the gas pressure within the RTG containment shell. In a vacuum, thermal radiation emitting from the RTG's fuel capsule surface is the only significant heat leak and this is minimized using multifoil insulation. As the gas pressure rises, the heat lost through the insulation via conduction becomes significant, resulting in a drop in the module hot side temperature. RTG tests indicate that the RTG electrical power output drops below 40 mW for a vacuum pressure greater than 5 mtorr. To maintain this 5 mtorr pressure limit, the RTG, especially the multifoil insulation, must be sufficiently outgassed and sealed such that residual outgassing and/or containment shell leaks after the RTG is fueled, do not result in a pressure above 5 mtorr throughout the RTG's operating lifetime. For the Pascal mission, the allowable leak rate is 1.2×10^{-9} torr · liters/sec.

Analytical studies show that an RTG open circuit can occur if excessive material vaporization of the module surface at elevated temperatures for long-term missions. The vaporizing leg material could undermine the gold tabs, which electrically connect the legs, thus increasing leg-tab resistance or causing an open circuit. Another concern has been that the condensable module vapor will condense on the module's lower temperature surfaces, creating a thin electrically conducting bridge between the module legs. Until now, RTGs have used modules with two or more parallel circuits to enhance RTG reliability. This sealed-off vacuum RTG uses a series circuit module, however; a parallel circuitry design is currently in progress.

RTG DESIGN

The RTG is designed around the 1 Watt Light Weight Radioisotope Heater Unit (RHU) which is used on U.S. spacecraft for localized heating of components (Tate, 1992). The RHU was designed and developed almost twenty years ago. It consists of a pellet of $^{238}PuO_2$ 6.3 mm (0.25 inch) in diameter and 9.4 mm (0.37 inch) long clad in 1mm (0.039 inch) thick Pt-30%Rh nested in a three-layer pyrolitic graphite insulating assembly enclosed in a carbon-carbon composite aeroshell for potential re-entry. Overall the RHU is 26 mm (1.02 inches) in diameter and 32 mm (1.26 inches) long, and its mass is 40 g. The thermoelectric module is 7.4 mm (0.29 inch) square in crossection and 22.9 (0.9 inch) in length. The RTG is 130 mm is 63.5 mm (2.5 inches) in diameter and 130 mm (6.0 inches) long, and its mass is 315 g in total. Design output for 1.0 W of heat from the RHU. The RHU power output declines $\cong$ 1%/year. Figure 1 illustrates the design up to its present stage and was previously presented (Allen, 2001).

RTG heat loss through the containment shell is limited to 14% of the RHU power by creating a vacuum and wrapping several packs of foil insulation around the RHU. Disk shaped insulation packs are also placed on both ends of the insulating cylinders. The insulation packs reflect the infrared radiation emitting from the 250 °C fuel capsule surface. These packs consist of a cylindrical wrap of alternating layers of Aluminized Kapton® and Cryotherm® micro-fiberglass paper (Bass, 1999). The insulation packs are bound together via a interlocking “saw-tooth” like weave at both ends of the insulation roll.

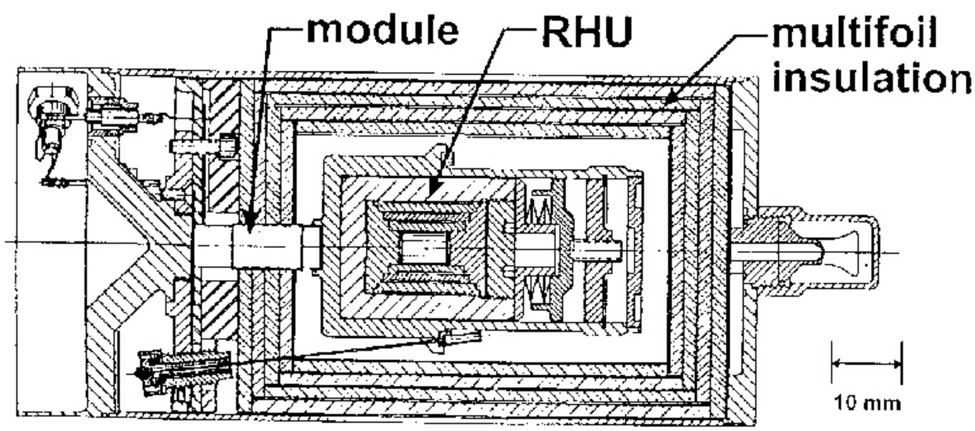

FIGURE 1. Milliwatt Radioisotope Power Supply

The tube on the top of the RTG (right side of Figure 1) is used to pump out the vacuum and then it is pinched-off to seal the RTG.

The thermoelectric module is composed of a 18 X 18 matrix of N and P type $(Bi,Sb)_2(Se,Te)_3$ legs, separated by a layer of Kapton®. Gold tabs at both ends of the module electrically connect the legs. Figure 2 illustrates the fuel capsule mounted on the module in an assembled RTG. To prevent an electrical short on either end of the module, a 1 millimeter layer of Kapton® is placed between the module - fuel capsule interface.

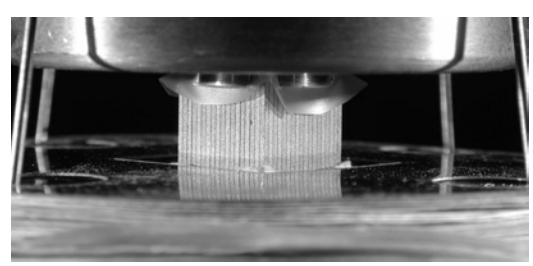

FIGURE 2. Fuel Capsule Mounted on Module with a Layer of Kapton® between the Module-Fuel Capsule Interface.

INSULATION OUTGASSING TESTS

Several outgassing tests performed on the multifoil insulation components indicate that the insulation does not degrade at elevated temperatures (250 °C) and sufficient pre-outgassing can be accomplished such that residual outgassing in a fully sealed RTG will not significantly effect the RTG vacuum.

Kapton® weight loss tests performed at DuPont indicate no weight loss after H_20 is removed. Figure 3 shows the weight loss of Kapton® in Helium and dry air vs. temperature. Significant weight loss begins at 475 °C, which is nearly double the operating temperature of the module hot side of 250 °C in the RTG.

Isothermal weight loss tests performed at DuPont on Kapton® in Helium and Air for several temperatures indicate insignificant weight loss under 400 °C.

An isothermal test performed on Kapton® (by Oak Ridge National Laboratory) by confirms Dupont's results. Figure 5 shows that the weight loss of Kapton® in a high vacuum is rapid initially but then slows substantially. Other experiments indicate that the Kapton® weight changes is due to water loss. Tests performed on the insulation micro-fiberglass paper at Hi-Z Technology also indicated insignificant weight loss after several hours in a furnace at 250 °C.

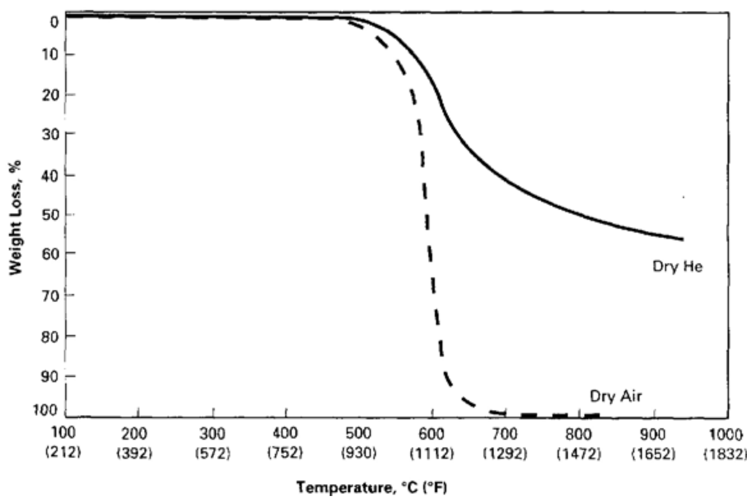

FIGURE 3. Kapton® Weight Loss in Helium and Dry Air.

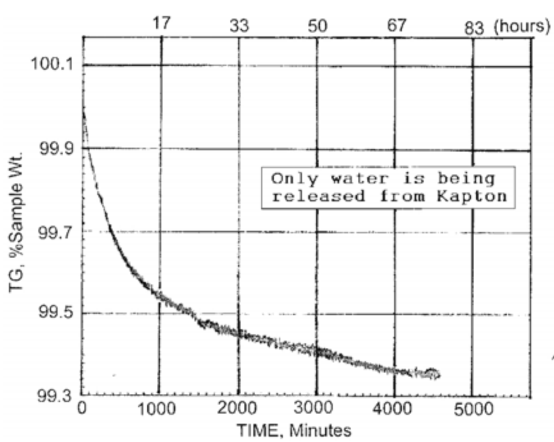

FIGURE 4. Kapton® Weight Loss in Helium and Dry Air for Several Temperatures.

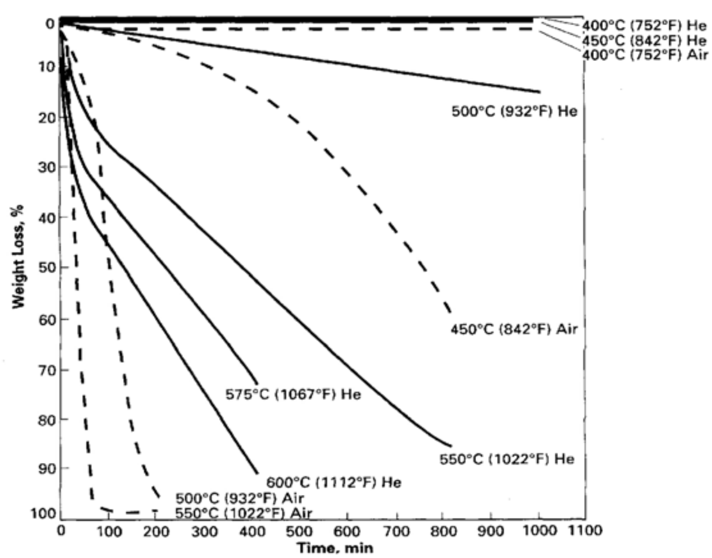

FIGURE 5. Kapton® Weight Loss at 250 °C.

Outgassing tests were performed in a high-vacuum system on two cylindrical insulation samples. Each of these samples consisted of alternate layers of Aluminized Kapton® and Cryotherm® 1303 paper wound together to make a roll. The amount of Kapton® and Cryotherm® 1303 paper in each sample was nominally the same as that contained within the generator. The high vacuum system included a residual gas analyzer and a valve for separating the test chamber from the pumping system. The entire vacuum system was outgassed at about 300 °C for several weeks prior to installation of a insulation sample. Figure 6 shows the outgassing results for Insulation Sample #2. The sample was outgassed in the test chamber for 21 days at a temperature between 250 °C and 270 °C.

Dry argon was introduced to the chamber and allowed to remain overnight. The next morning, the argon was pumped from the chamber, which was then heated to 150 °C. The high vacuum valve was closed to examine the influence of the insulation on chamber pressure as a function of time. The results are shown in Figure 6. After about 75 hours, the test chamber was heated to 250 °C, which caused the pressure to increase to about 3 x 10^{-5} torr. The pressure in the test chamber slowly dropped with increasing time. Results from the RGA indicate that the decreasing pressure with time is caused by a slow reduction in argon pressure. As shown in Figure 6, the system pressure with Sample #1 after it was heated to 250 °C is in excellent agreement with the results from Sample #2. Results from both samples indicate that the insulation can be outgassed and exposed to dry argon without significantly contributing outgassing products to a closed system. The final pressure observed with both samples is a factor of 200 below the 5 millitorr limit required and there is no reason to suspect that longer time exposure will lead to problems.

.

These tests were not identical to actual RTG operating conditions because the volume of the chamber was 5 times larger than the RTG volume and the temperature of the insulation packs were isothermal whereas in an operating RTG the insulating layers vary from 50 °C (outermost insulating layer) to 240 °C (innermost insulating layer). These mismatched operating conditions tend to compensate one another because the volume difference suppresses the pressure rise rate whereas the uniform temperature across the insulation pack tends to increases the pressure rise rate.

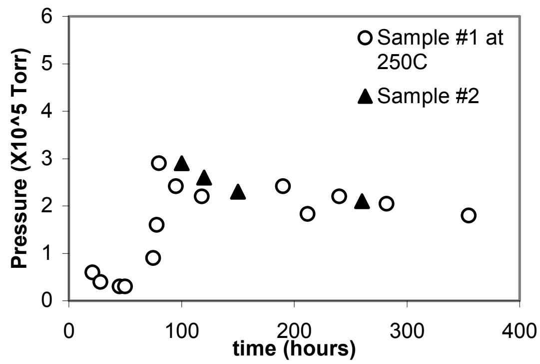

FIGURE 6. Vacuum Chamber Pressure vs. Time Curve With and Without the RTG Insulation.

To prevent the insulation from acting as a getter after being outgassed and during transportation from the furnace to the RTG, high-purity Argon will be used in a glove box during Insulation loading into the RTG. Further tests are currently underway to determine the amount of residual Argon outgassing after the insulation is loaded into the RTG.

N AND P TYPE VAPORIZATION TESTS

Isothermal weight loss tests conducted on the N and P-type semiconductors indicate insignificant weight loss in the N-type and a slowly decreasing weight loss rate of the P-type with time. Mass spectrometer vapor pressure measurements performed on N and P type samples at General Atomics in the 1970's revealed that Te_2 has a vapor pressure approximately one order of magnitude greater than any other species in the samples.

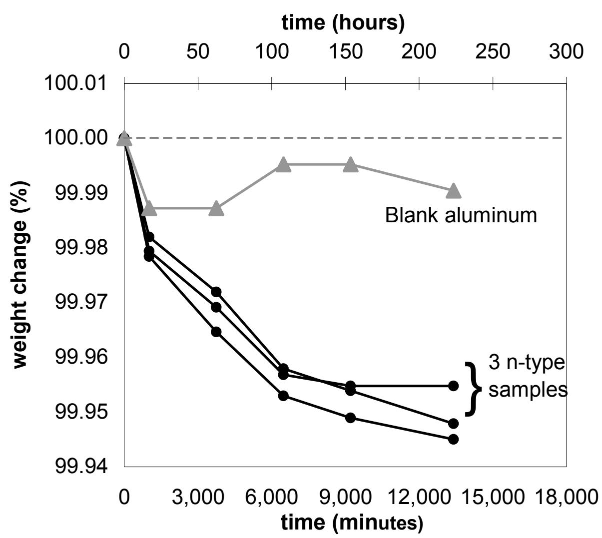

FIGURE 7. Weight Loss of N-Type at 255 °C.

The N-type sample (Bi_2Te_3-12%Bi_2Se_3) weight loss rate becomes insignificant after 220 hours as indicated in Figure 7. SEM analysis of the sample surface and center of a cleaved edge indicate an enriched concentration of Selenium possibly in the form of Bi_2Se_3 as Te_2 vaporizes from the sample surface as shown in Table 1. Since Bi_2Se_3 is more stable than Bi_2Te_3 (free energy of formation is higher), its vaporization rate (i.e. Se_2 will be the highest vapor pressure component) is probably lower. This behavior is not unusual for group VI elements, O, S, Se, & Te. These compounds typically increase in their thermal stability as one goes from the Tellurides to the Selenides to the Sulfides to the Oxides. The enriched Bi_2Se_3 surface appears to act as a baffle, suppressing further Te_2 vaporization.

TABLE 1. SEM Analysis of N-Type Sample Surface and Center of Edge.

N-Type Sample after 650 hours @ 255 °C	Element	Center	Surface	% Change
	Te	52.8 %	51.4 %	- 3 %
	Bi	39.8 %	38.4 %	- 1 %
	Se	7.4 %	10.2 %	**+ 38 %**

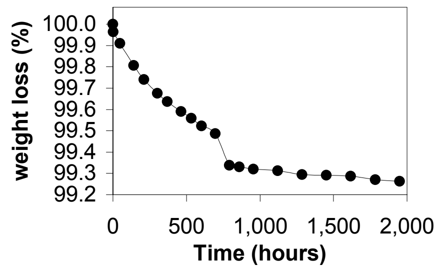

FIGURE 8. WeightLoss of P-Type @ 255° C

The P–type sample (Sb_2Te_3 – 22%Bi_2Te_3) weight loss rate reduces With time but continues to drop after 2000 hours as indicated in Figure 8. The average furnace temperature during the first 800 hours of the test was 254 °C, and 252 °C during the last 1200 hours. Although the weight loss rate is sensitive to temperature, the difference in weight loss rate due to the 2-degree discrepancy is insignificant.

Similar weight loss tests performed at ORNL indicate similar results for both N and P type samples. It can be shown that the vapor pressure data of N and P type samples recorded at General Atomics (Elsner, 1971) closely agree with the initial weight loss rates of the Hi-Z furnace samples by using the equation (1) which equates a species vapor pressure to it's weight loss rate per unit area per unit time (Dayton, 1998) and equation (2) which is a curve fit of GA's vapor pressure measurements.

$$G = \frac{P_t}{17.14}\sqrt{\frac{M}{T}} \tag{1}$$

$$P_t = 10^{(7.31-9666/T)} \tag{2}$$

Module Vaporization Model

A 2-d surface profile model of a single P-type leg has been developed to better understand the negative effects that vaporizing legs can have on module power output and reliability for long-term missions. The model is representative of a leg exposed to a vacuum on 2 of its 4 vertical surfaces. At the hot junction, the edge of a leg of a module, experiences 2-d vaporization because they are baffled on 3 of their 4 vertical sides by adjacent legs. The inner legs are mostly baffled by the Kapton® film located between the fuel capsule and module hot side. The edge legs are partly baffled by the Kapton® film, whereas with this model it is assumed they are completely exposed to the vacuum so that the worst-case scenario can be analyzed. The model assumptions are stated below:

Model Assumptions

I. The leg is composed of pure Te_2, thus Te_2 is the only element vaporizing from the leg surface. The other vapor pressure species (BiTe, Bi) have vapor pressures that are one order of magnitude smaller than Te_2 for the temperature range in which the module hot side will be operating under (210< 250 °C).

II. The weight loss rate per unit area (vaporization rate) of a given surface area element dA on the leg is determined by its temperature and surface area exposure to the vacuum. Equation (1) and (2) are used to calculate the weight loss rate for a given surface element temperature. Curved surfaces and sharp corners area elements have a weight loss rate proportionately greater than a flat area element at the same temperature. This proportionality constant is determined by the amount of element area exposed to the vacuum. This assumption neglects: 1) the increasing surface area of the leg caused by the increasing surface roughness associated with a vaporizing surface, and 2) baffles that may suppress vaporization such as the Kapton® film that overhangs the module hot side after the RTG is assembled.

III. The temperature gradient is linear from the hot to cold side of the leg. The slope of this gradient reduces over time due to the decreases in RHU power output each year. In this assumption the 14 % RHU heat loss, caused by radiation emitted from the fuel capsule surface, is assumed constant. The heat lost by radiation is proportional to T^4, thus proportionately less of the RHU heat would be lost by radiation as the temperature of the hot side decreases, which would cause the hot side of the module to remain at slightly higher temperatures than the yearly linear temperature drop assumption predicts.

IV. The temperature is uniform throughout any horizontal cross section of the leg.

Model Results

The 2-d surface curves for the hot side of a 0.9" X 0.015" X 0.015" leg is shown in Figures 9 (a – f). In each figure the outermost surface line represents the surface of the leg time zero. The proceeding surfacing curves (outer → inner) represent increments of 5 years.

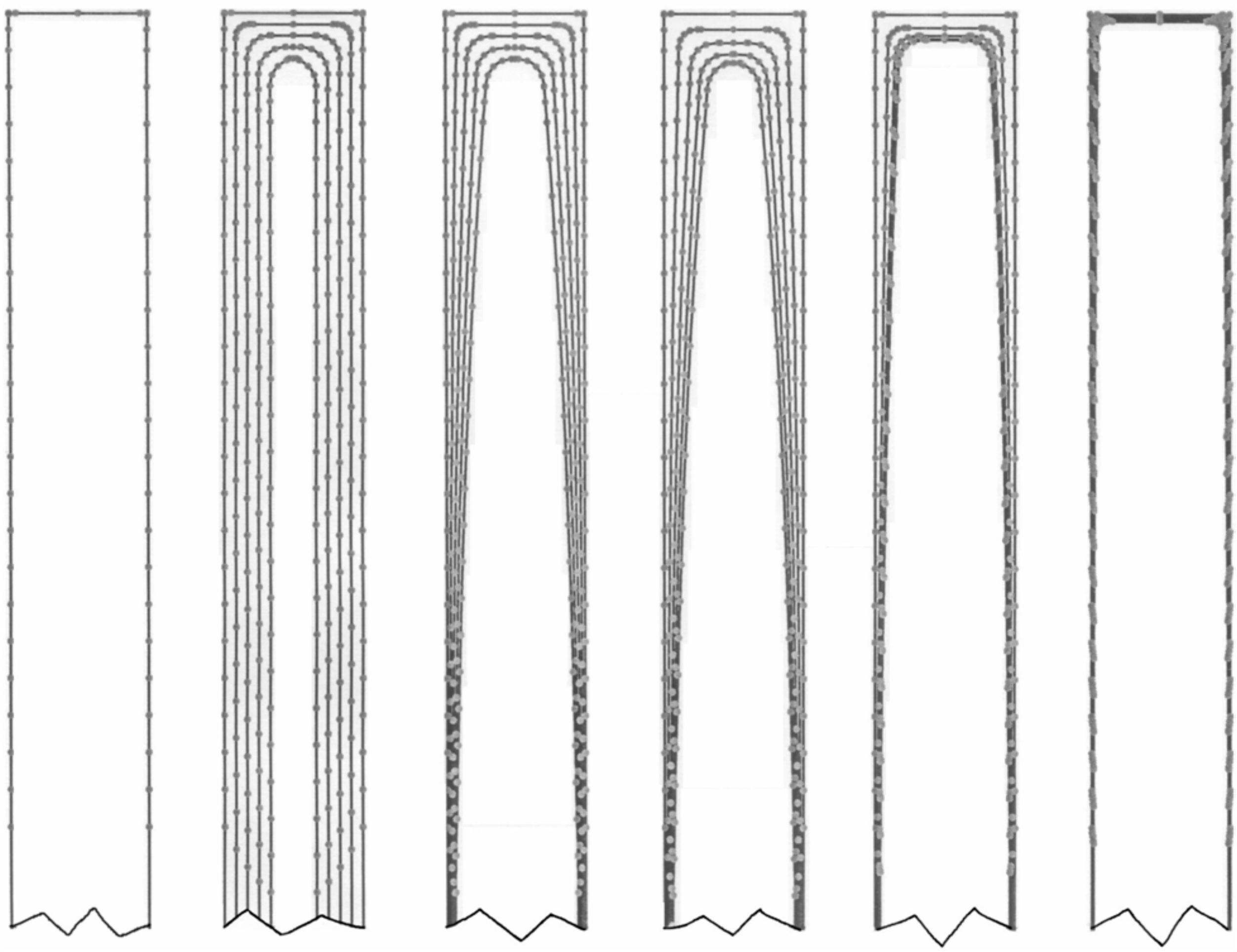

a)	b)	c)	d)	e)	f)
Th = 50 °C	Th = 245 °C	Th = 245 °C	Th = 250 °C	Th = 250 °C	Th = 250 °C
Tc = 50 °C	Tc = 245 °C	Tc = 50 °C	Tc = 50 °C	Tc = 50 °C	Tc = 50 °C
Decay = 0%	Decay = 0 %	Decay = 0 %	Decay = 0.1 %	Decay = 0.3 %	Decay = 1.0 %

FIGURE 9. 2-D Surface Profile of Leg Hot Side as a Function of Initial T_{hot}, T_{cold}, and RHU Power Decay Rate. Scale 50 X 1.

All of the surface lines in Figure 9a overlap the time zero curve because the hot and cold side are only 50 °C (no vaporization). The surface lines in Figure 9b are parallel and equally spaced because the RHU decay rate was set to zero and the both the hot and cold side temperatures of the leg are set to 245 °C. In Figure 9c the lines converge towards the time zero surface away from the hot side surface because a temperature gradient exists between the hot and cold side of the leg. The lines are evenly spaced for a given horizontal leg cross section because the RHU decay rate was set to zero, thus the hot side temperature remains constant. In Figure 9d the RHU decay rate is set to 0.1%, causing a proportionately uniform drop in leg surface temperature with time. The effects of the uniform temperature drop is seen by the decrease in surface line spacing with time. The RHU decay causes the spacing of the surface lines to reduce with time, thus the rate of material removal form the leg surface decreases with time. In Figure 9e The RHU decay rate is increased from 0.1% to 0.3 %, resulting in more closely spaced surface lines – less material is vaporizing with time. And final Figure 9f is shows the surface lines with the RHU decay rate of the actual decay rate of 1%. Note that an only a fraction of the leg material vaporizes as compared to Figure 9d which had a RHU decay rate of 0.1%.

The significant changes in material vaporizing from the leg surfaces in Figure 9 is due to the exponential dependence of surface weight loss rate on surface temperature. In Figure 9d the hot side temperature is 246 °C after 20 years because the RHU decay rate was set to only 0.1%, whereas in Figure 9f the hot side temperature is 210 °C after 20 years because the RHU decay rate was set to 1%. From equation (1) and (2) the exponential dependence of weight loss rate (G) on temperature can be determined and is shown in Figure 10. The weight loss rate at 250 °C is 2.4 times the weight loss rate at 240 °C, which results in a 56% drop in weight loss rate on the leg surface hot side after the first five years. After 10, 15 , and 20 years the weight loss rate drops by 81%, 92%, 97% respectively.

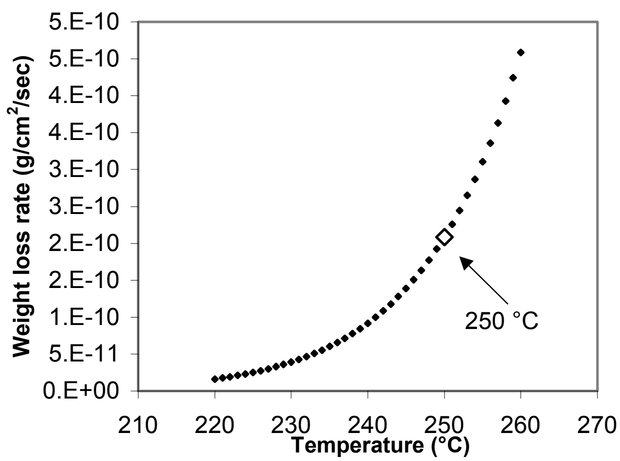

FIGURE 10. Te_2 Weight Loss Rate as Function of Temperature.

To validate this vaporization model, a module has been placed under accelerated test conditions at Hi-Z. In this test the module is in a vacuum and has hot and cold side temperatures of 300 °C and 50 °C respectively. The additional 50 °C on the module hot increases the vaporization rate by a factor of 40, simulating 20 years of vaporization in 6 months.

Effects of Module Vaporization

If the amount of material vaporized from a module leg is significant, the modules power output can be effected by: 1) increased module resistance or open circuit due to "tunneling" underneath the gold tabs, 2) module electrical short due to vapor condensing on the lower temperature module surfaces which can form an electrically conductive bridge between legs, and/or 3) a reduction in the foil insulating effectiveness due to a increase in the foil emissivity caused by vapor condensing on the lower temperature foil surfaces.

A module electrical short due to "tunneling" underneath the gold tabs is unlikely after 20 years of operation because the 20 year surface line in Figure 9f is relatively close to the original leg surface (time zero surface). It should also be noted that the severity of "tunneling" underneath the gold tabs is dependent upon the size of the tabs, which is determined by the leg cross sectional area. If the leg width in Figure 9f were reduced to 1/10 of its value, the "tunneling" underneath the gold tabs would be severe and likely cause a module open circuit.

A module is currently on test at Hi-Z to determine the decrease in module resistance due to the thin electrical conductive bridge forming between leg surfaces as Te vapor condenses on the module cooler surfaces. This test is running with a hot side of 300 °C, which accelerates the test by a factor of 40, thus a 20-year test will be completed in 6 months. After 2 months under test (7 accelerated years), the module surface is showing discoloring, however the module resistance remains constant (Figure 11). The module surface color becomes uniformly darker with increasing proximity to the cold side.

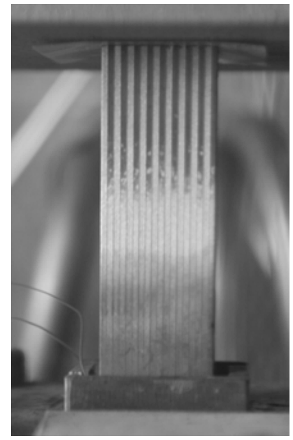

FIGURE 11.

Module Vaporization Suppression Techniques

As indicated by the module vaporization model (Figure 9), there is not a significant amount of Te_2 vaporizing from any of the module legs to cause concern. However; several vaporization suppression techniques have been identified that can be used to suppress weight loss under higher module operating temperatures: 1) adding selenium to the P type material in place of some Te, 2) using a Kapton® film baffle on the hot side of the module, and 3) connecting the module legs in a parallel circuit such that one or two disconnected gold tabs will result in less then 1% decrease in module power output.

In any event the Kapton® film will be used as the hot side electrical insulator between the module and the heat source housing (fuel capsule). Evaluation of this concept is underway.

Several ½ watt Modules bonded with epoxy have operated in Xenon for 15 years. An SEM image of the a 15 year module edge legs indicates little vaporization as shown in Figure 12. Similar baffling techniques on the 40-mw module may result in similar module vaporization.

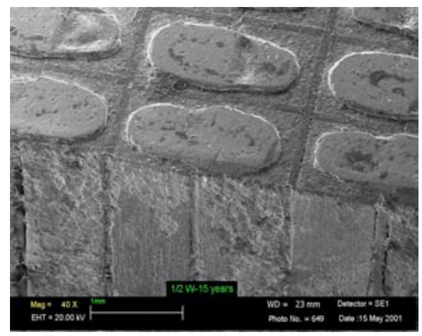

FIGURE 12.

CONCLUSIONS

The data generated thus far indicates the vacuum insulation can be sufficiently outgassed at some required temperature, transferred to an Argon glove box, and loaded into the RTG. The only outgassing species identified thus far is water and given sufficient time/temperature it can be removed from the Kapton®.

Experimental data and vaporization models indicate that module vaporization does not significantly affect RTG power output for an operating period of 20 years that begins with a Th of 250 °C and slowly drops in temperature due to fuel decay.

The first prototype RTG will be assembled at Mound laboratory in their Argon glove box. This first unit will help provide valuable information regarding the pumpout time required to achieve a stable vacuum.

ACKNOWLEDGEMENT

Hi-Z would like to acknowledge and thank the U.S Department of Energy, Office of Space and Defense Power Systems, for their funding and program support of the 40 mW RTG program.

REFERENCES

Allen, Daniel T., "Millwatt Radioisotope Power Supply for the PASCAL Mars Surface Stations," in proceedings of *Space Technology and Applications International Forum (STAIF-2001),* edited by M. El-Genk, AIP Conference Proceedings, New York, 2001.

Bass, John C., and Daniel T. Allen "Millwatt Radioisotope Power Supply for Space Applications," in proceedings of *18Th International Conference on Thermoelectrics (1999),* edited by C. Vining, Institute of Electrical and Electronics Engineers, Inc., New Jersey, 1999, pp. 521-524.

Dayton, Benjamin B., "Kinetic Theory of Gases," in Foundations of Vacuum Science and Technology, edited by James M. Lafferty, John Wiley & Sons, Inc., 1998, pp. 23.

Zimmerman, W., Bryant, S., Zitzelberger, J., and Nesmith, B., "A Radioisotope Powered Crybot for Penetrating the Europan Ice Shell," in proceedings of *Space Technology and Applications International Forum (STAIF-2001),* edited by M.S. El-Genk, AIP Conference Proceedings, New York, 2001, pp. 707-715.

Elsner, N. B, Rovner, L.H., and Staley, H. G., "Bismuth Telluride Converter Fabrication Technology," Gulf General Atomic Project 0027.0000, GAMD-11021, Gulf General Atomic Company, 1971, pp. 20.